A Miniaturized Omni-directional Negative Permittivity Zeroth-Order Resonance Antenna

Ming-Chun Tang [1], Tianwei Deng [2], Han Xiong [1], Shaowei Qing [3], and Hao Zeng [1]

[1] College of Communication Engineering
Chongqing University, Chongqing 400044, China
tangmingchunuestc@126.com, xiong1226han@126.com, haoz@cqu.edu.cn

[2] Department of Electrical & Computer Engineering
National University of Singapore (NUS), 119077, Singapore
tsldt@nus.edu.sg

[3] Power Engineering Institute
Chongqing University, Chongqing 400044, China
qshaowei@gmail.com

Abstract ─ An Evolved Negative permittivity (ENG) Zeroth-Order Resonance (ZOR) antenna with miniaturized size and ultra-low profile is presented in this paper. By adding parasitic patch and loading meander line in steps, the antenna ZOR operational frequency is decreased from 5.084 GHz to 177.8685 MHz, while keeping the overall dimensions unchanged; which is equivalent to about twenty-eight times electrical size reduction based on the equivalent circuit models. Moreover, the proposed miniaturized antenna with omni-directional radiation performance is promising for the specific low-power radio applications, such as short range remote control system and household security system.

Index Terms ─ Evolved negative permittivity, low-profile, miniaturization, zeroth-order resonance antenna.

I. INTRODUCTION

With the ever increasing demand for compact wireless communication system, which includes mobile and Wireless Local Area Network (WLAN) systems, miniature antenna has gained significantly more attentions in recent years. In order to achieve antenna miniaturization, lots of effective techniques have been proposed since the fundamental limitations of miniature antennas were theoretically explored since 1940's [1-2]. Hitherto, examples of antenna miniaturization techniques include using Genetic Algorithms (GA) method [3-4]; resorting to meander or Peano line [5-6], reactive/slot loading [7-12], negative permittivity (ENG)/negative permeability (MNG) Metamaterial (MTM) shells [13-16] and left-handed Transmission Lines (TL) loadings [17]. Employing high dielectric constant [18], magneto-dielectric [19], Artificial Magnetic Conductor (AMC) [20] and MNG metamaterial [21] substrates; utilizing Split-Ring Resonator (SRR) structures [22-23] and applying the MTM TL approach. For particular interest, miniature antennas based on MTM TL approach have drawn much attention and were extensively reported for their unique performance resulting from the rich dispersion of MTM TL materials. Generally, these MTM TL based antennas could be classified into the following three categories: Composite Right/Left Handed (CRLH) antennas [24-26], MNG Zeroth-Order Resonance (ZOR) antennas [27] and ENG ZOR antennas [28-32]. All of these MTM TL antennas could function in ZOR mode, which is independent on its physical length. However, as is known, the overall configurations of the metamaterial unit are quite crucial for their performance, while satisfying the

Submitted On: October 30, 2013
Accepted On: June 28, 2014

demands in specific applications, such as radiation gain, bandwidth and miniaturization level. On one hand, in order to improve the radiation gain, a special MTM TL metamaterial with equilateral slots on ground plane, which makes the resonator store less electromagnetic energy in the zeroth-order mode, was reported in [25]. On the other hand, the bandwidth of the MTM TL antennas has been distinctly broadened with the aid of mushroom structure [29]. However, up to now, there was little literature to comprehensively discuss how to achieve the further electrical reduction of MTM TL based antenna.

In this paper, according to the equivalent circuit models, a miniature ENG ZOR antenna with the overall dimensions $0.00954\lambda_0 \times 0.00954\lambda_0 \times 0.000475\lambda_0$ (where λ_0 is the wavelength corresponding to the operational frequency f_0 in free space) is successfully designed and manufactured, via an evolution of a traditional ENG ZOR antenna by following two effective steps: (1) additional capacitance was created by resorting to the virtual ground and (2) by etching meander-line, additional inductance and capacitance were obtained.

II. AN ENG ZOR ANTENNA DESIGN

According to the literatures [28-32], a compact one-unit-cell ENG ZOR antenna was constructed and the topology is shown in Fig. 1. In this design, a substrate with the thickness of 0.8 mm, relative dielectric constant ε_r=3.38 and loss tangent tanδ=0.0007 is selected. Considering the input resistance for these types of antennas is inherently much higher than the characteristic impedance of feed line [28-29], a feeding gap is employed so that the high input resistance could be reduced to match the 50 Ω characteristic impedance. The configuration was numerically simulated using Ansoft HFSS (a commercial electromagnetic solver based on finite element method) [33]. The results in Fig. 2 demonstrate that the proposed ENG antenna operates in the center of 5.084 GHz, which is corresponding to the overall dimensions of $0.273\lambda_0 \times 0.273\lambda_0 \times 0.0136\lambda_0$. As has been proven in [28], for such ENG antenna, the ZOR mode resonance frequency serves as the lowest operational frequency.

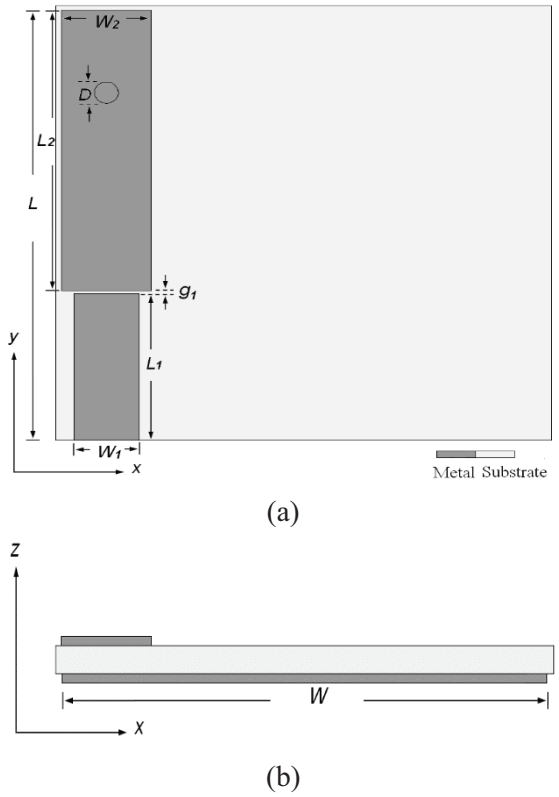

Fig. 1. Proposed ENG ZOR antenna: (a) front view and (b) side view. The dimensions in mm are: L=16.08, W=16.08, L_1=5.49, W_1=2.18, g_1=0.11, L_2=10.48 and W_2=3.

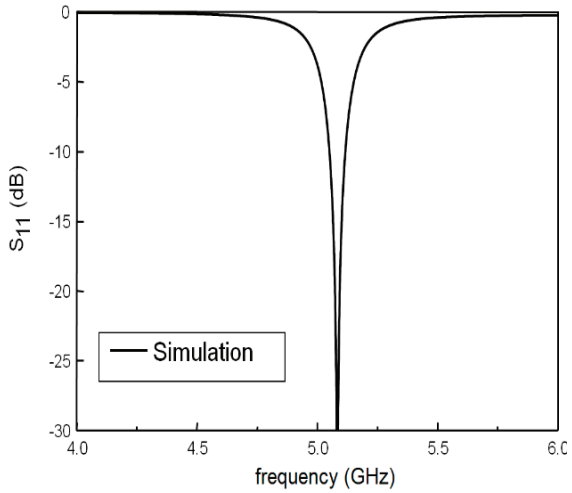

Fig. 2. Simulated reflection coefficients of ENG ZOR antenna.

Figure 3 gives the topology of equivalent circuit model for the proposed ENG ZOR antenna

based on [28-32]. In the model, C_0 is the couplingcapacitance between patch and feed line. The part in the dot region of the model indicates one unit cell of ENG MTM TL. L_R and C_R are the inherent distributed inductance and capacitance for the traditional Right Handed (RH) TL, L_{Lv} is the shunt inductance provided by the grounded via and G is the conductance. The equivalent circuit parameters which are extracted from the simulation data for the unit cell (in Fig. 2) are: C_0=0.0124pF, L_R=78.75nH, G=1/(1.64×10^6)S, L_{Lv}=0.92nH, C_R=1.06pF and Z_{in}=50Ω, respectively. The zeroth-order resonance frequency of $f_0=1/(2\pi\sqrt{L_L C_R})$ is related to the size of rectangular patch and the length of via, which determine the values of C_R and L_L [28], respectively. Moreover, according to our simulation, it was found that the ground size has significant impact on the antenna radiation characteristics; especially the gain performance.

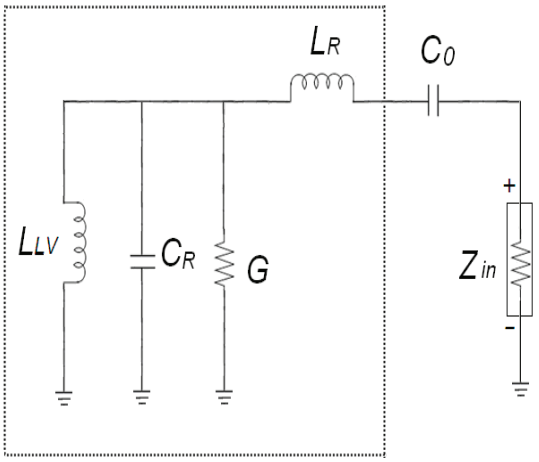

Fig. 3. Topology of the equivalent circuit for the traditional ENG ZOR antenna.

III. EVOLVED ENG ZOR ANTENNA DESIGN

A. Parasitic patch loading technology

As the first step for the evolution of traditional ENG ZOR antenna, we resort to loading a parasitic patch near the radiating one. Figure 4 illustrates the design of ENG ZOR antenna. The other parameters keep the same as the traditional ENG ZOR antenna (shown in Fig. 1). In the design, the meander line and parasitic patch are, respectively, added to accomplish shunt inductance and virtual ground capacitance [34].

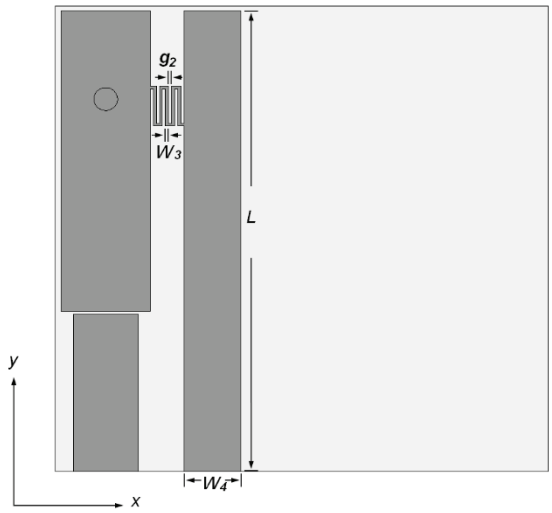

(a)

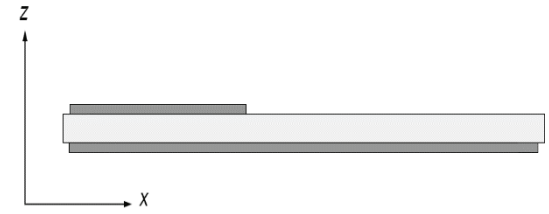

(b)

Fig. 4. ENG ZOR antenna loaded with virtual ground: (a) front view and (b) side view. The dimensions in mm are: L=16.08, g_2=0.1, W_3=0.1 and W_4=0.2.

Here, the influence of the parasitic patch on the ZOR frequency has been numerically investigated, shown in Fig. 5. By changing the width of parasitic patch (W_4), the operational frequency bandwidth, the resonance frequency position, the resonance strength of ENG ZOR antenna changed accordingly. Obviously, when the width goes larger, the ZOR operational frequency would shift lower. The reason is that the virtual ground capacitance is directly influenced by the position and dimension of parasitic patch [34]. Based on this principle, when the width alters from 2 mm to the maximum 12.06 mm, the virtual ground capacitance goes larger, further leading ZOR operational frequency

to decrease from 1.9090 GHz to 0.9807 GHz. Meanwhile, its radiation impedance also varies with W_4, making the antenna not match well with the characteristic impedance 50 Ω (especially when W_4=12.06 mm), since the antenna is fed using capacitively coupling technology. Therefore, adjusting the gap width (i.e., coupling capacitance C_0) between radiation patch and feed line, (g_1) is implemented for accommodation.

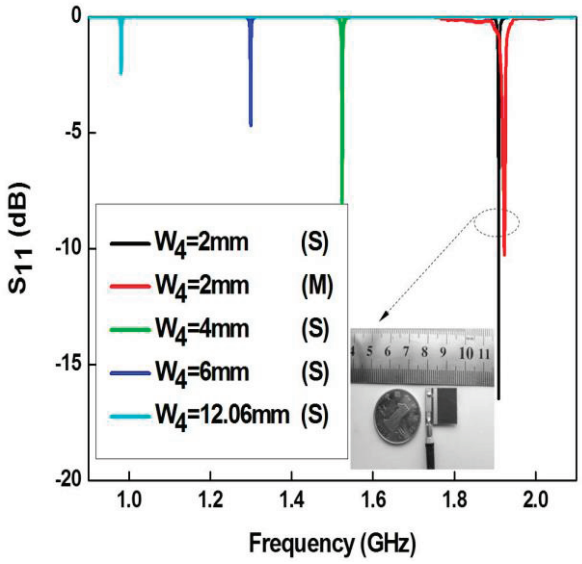

Fig. 5. Simulated and measured reflection coefficients of ENG ZOR antennas with virtual ground (notation "S" and "M" indicate the simulated and measured results, respectively.)

And then, in order to validate the simulation results, the measurement (when W_4=2 mm) is also carried out using AV3618 Vector Network Analyzer (VNA). As illustrated in Fig. 5, the measured results are generally in agreement with the simulation with an acceptable operational frequency drift (only 0.73% higher shifting). Meanwhile, the simulated and measured peak realized gains witness 0.91 dB difference, shown in Table 1. Also, it could be concluded from simulation results summarized in Table 1 that when the ZOR operational frequency decreases, the Q increases accordingly, which would result in a certain decrease of the antenna peak realized gain.

Table 1: Influence of width of parasitic patch on ZOR operating frequency and peak gain

Width of Parasitic Patch W_4 (mm)	ZOR Operating Frequency (GHz)	The Corresponding Electric Length ($\lambda_0\times\lambda_0\times\lambda_0$)	Peak Gain (dBi)
2	1.9090 (S) 1.92 (M)	0.1028×0.1028×0.00509 (S) 0.1036×0.1036×0.00513 (M)	-7.32 (S) -8.23 (M)
4	1.5324	0.0825×0.0825×0.00409	-9.4358
6	1.2989	0.0699×0.0699×0.00346	-10.90
12.06	0.9807	0.0528×0.0528×0.00262	

B. Meander line loading technology

Usually, meander-line designs were applied to produce both capacitance and inductance for wire antennas, which enable the antennas with much smaller electrical size [35-37]. At this step, the technique of etching periodic slots to design meander line on the ground is carried out to accomplish the ENG ZOR antenna further miniaturization. Figure 6 shows the evolved antenna design. As was already demonstrated in Table 1, the maximum width of parasitic patch (W_4=12.06 mm) is selected to reach the lowest frequency, ensured by virtual ground capacitance. Here, the periodic thin meander line is constructed vertically below the parasitic patch in order to obtain the additional inductance and capacitance, hoping for further miniaturization.

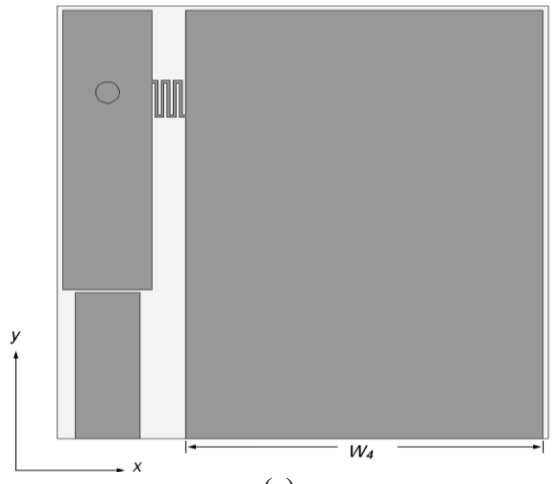

(a)

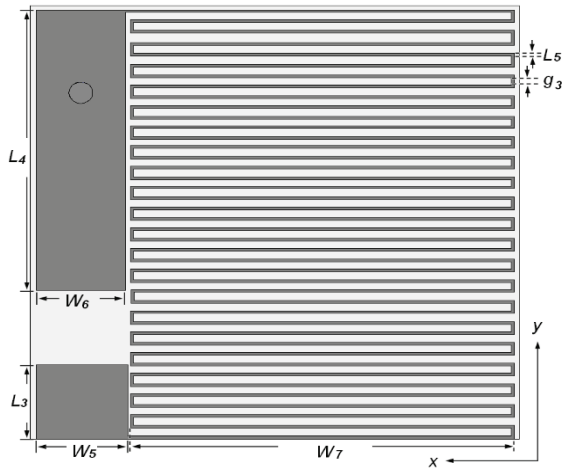

(b)

Fig. 6. The ENG ZOR antenna etched with meander line: (a) front view with the dimensions: W_4=12.06 mm and (b) back view with the dimensions in mm: L_3=2.8, W_5=3.09, L_4=10.05, W_6=3, L_5= 0.1, g_3=0.28 and W_7=12.94.

The simulation results from HFSS are described in Fig. 7. From this result, it is obvious that the operational frequency of proposed ENG ZOR antenna is successfully lowered from 980.7200 MHz to 177.8685 MHz with good impedance matching (S_{11}=-26.55 dB). Meanwhile, the peak realized gain drops (with the maximum -29.97 dBi at the operational frequency center). It is reasonable that the ZOR operational frequency is lowered dramatically at the expense of narrow bandwidth and low gain [37].

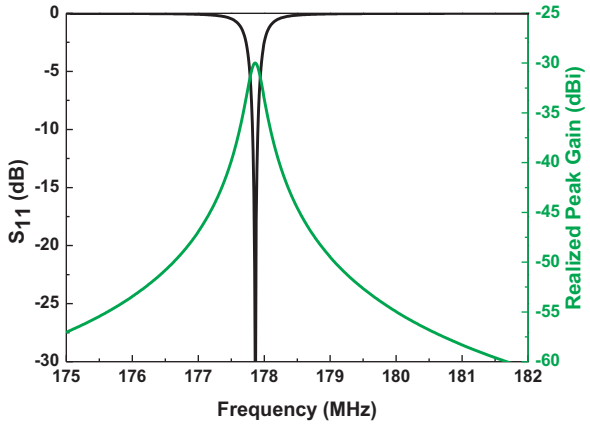

Fig. 7. Simulated reflection coefficients and peak gain of ENG ZOR antennas with meander line.

In order to further investigate the radiation performance, the HFSS simulated gain patterns in the far field are shown in Fig. 8. Generally, the pattern resembles that of a monopole; nearly omni-directional in the *Z-X* plane and bi-directional in the *Z -Y* plane.

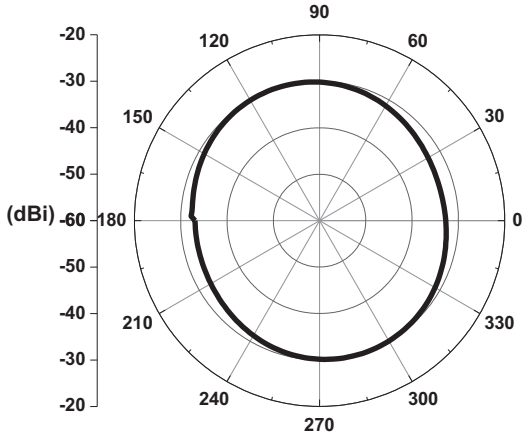

(a)

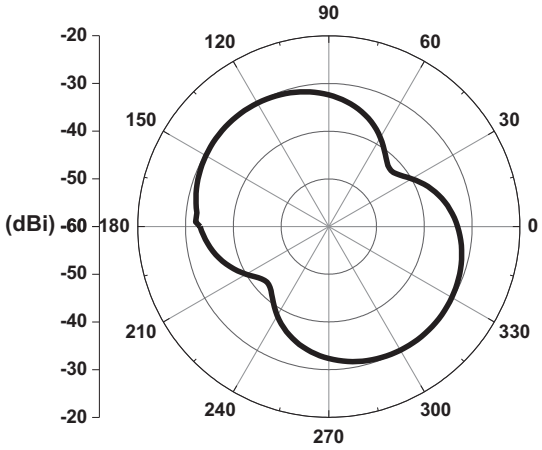

(b)

Fig. 8. Simulated gain pattern of ENG ZOR antennas with meander line at lowest operational frequency center 177.8685 MHz: (a) in *Z-X* plane and (b) in *Z-Y* plane.

Furthermore, the effect of meander line (at the bottom of the substrate) has been analyzed in Fig. 9. When the antenna operates at ZOR frequency, the majority of current concentrates on the meander line, indicating its significant contribution on radiation performances. In details, two amplified current distribution images

(I) and (II) were presented to explain the physical mechanism of Figs. 7 and 8. From the middle part in image (I), the transverse currents polarized along the *x*-direction on the meander line. On the whole, as their effect on the far-field radiation pattern can be counteracted, due to the opposite-phase polarizations of the nearby sections, it would give little contribution to the far-field radiation power [36, 37]. Meanwhile, at the edge of meander line in image (II), the currents on the sections, which are in parallel with *y*-direction, exhibit the almost in-phase polarizations of nearby sections along the *y*-direction [37]. Likewise, the sum of all of the sections (in the *y*-direction) act as a continuous line source located along *y*-direction, which thus, contribute bi-directionally in the *Z-Y* plane and nearly omni-directional radiation pattern in the *Z-X* plane. Above analysis of the phenomenon presents the reason for the simulation results in Fig. 8.

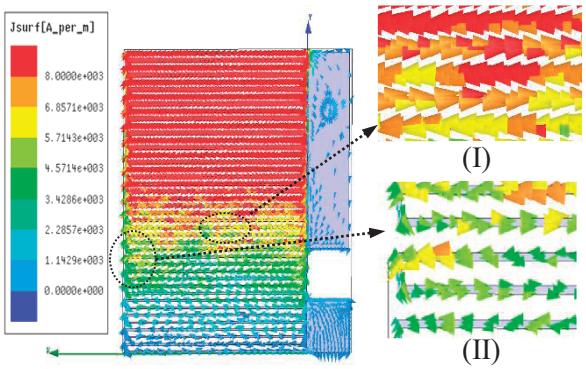

Fig. 9. Current distributions on the meander line of the evolved ENG ZOR antennas.

In the same way as Fig. 3, a topology of equivalent circuit model for the evolved ENG ZOR is shown in Fig. 10. In the similar behavior, C_0' indicates the coupling capacitance between patch and feed line in the model, the part in the dot region of the model presents one unit cell of evolved ENG MTL transmission line; L_R' and C_R' are the distributed inductance (including meander-line inductance) and capacitance (including meander-line capacitance and the capacitance between meander-line and parasitic patch) for the traditional Right Handed (RH) TL, L_{LV}' is the shunt inductance provided by the grounded via and G' is the radiation conductance. Moreover, L_{Lg} and C_g represent the shunt inductance provided by the meander line in the middle of two patches and the capacitance provided by virtual ground, respectively. Finally, the equivalent circuit parameters extracted from the simulation data of the unit cell (in Fig. 6) are: C_0'=0.0124pF, L_R'=64591.4nH, L_{LV}'=373.31nH, C_R'=63.56pF, L_{Lg}=39.7176nH, C_g=34.377pF, G'=1/(6.62×10^8)S and z_{in}=50Ω, respectively.

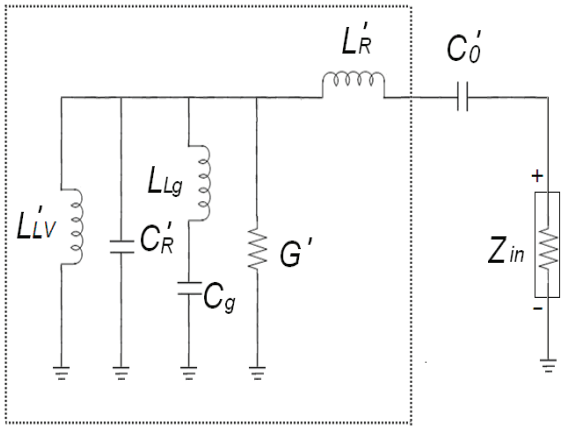

Fig. 10. The equivalent circuit model for the evolved ENG ZOR antenna.

Based on literatures [28, 34], the corresponding ZOR frequency of our proposed antenna is determined by the following equation:

$$f_0' = \frac{1}{2\pi}\cdot\sqrt{\left[\left(\frac{L_{Lv}L_{Lg}}{L_{Lv}+L_{Lg}}\right)C_R\right]^{-1}+\left[\left(\frac{L_{Lv}L_{Lg}}{L_{Lv}+L_{Lg}}\right)C_g\right]^{-1}} \quad (1)$$

From equation (1) and above analysis for each component parameters, it can be concluded that f_0' is related to the sizes of radiating and parasitic patches, the dimensions of meander lines and the length of via. In other words, while the overall dimensions of the antenna remain the same, the position of f_0' could be easily adjusted in a very large frequency region (from 177.8685 MHz to 5.084 GHz) by changing certain components in suitable dimensions.

IV. MEASUREMENT

Furthermore, the miniaturized antenna has been constructed and fabricated and the

measurement has been implemented to validate the simulation and equivalent circuit results, as shown in Fig. 11. Figure 12 shows the measured reflection coefficient of evolved ENG ZOR antenna. Obviously, the measured ZOR antenna operates at 179.48 MHz that is a little higher (~ 2 MHz shift) than that of simulation and also shows a good impedance match (S_{11}=-14.75 dB). It deserves to mention that these considerable discrepancies for such miniature antenna could be tolerable as well [12]. In addition, we note that since the peak gain of this type antenna is quite low (~-30 dBi), the Signal to Noise Ratio (SNR) in the measurement carried out in our current anechoic chamber should be very low, which the measurement setup could not reflect its radiation performance characteristics accurately. Thus, the measured radiation performances of proposed antenna were not reported here.

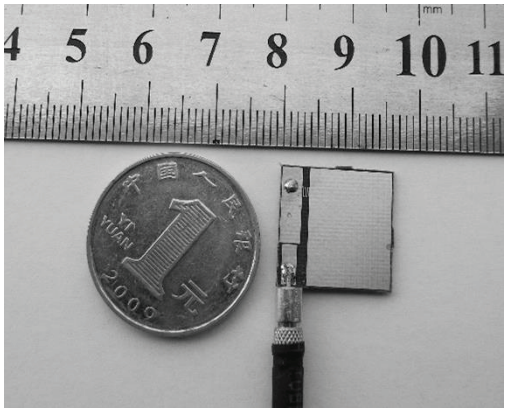

(a)

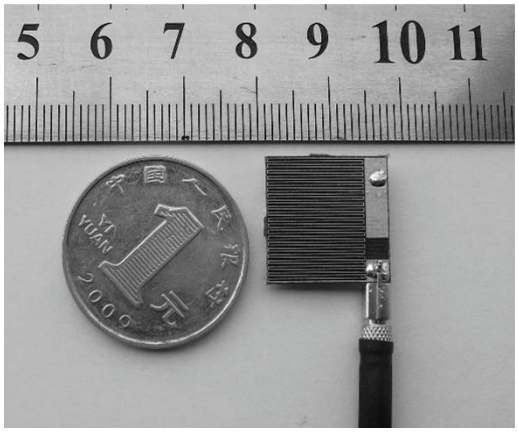

(b)

Fig. 11. Photograph of the fabricated evolved ENG ZOR antenna: (a) front view and (b) back view.

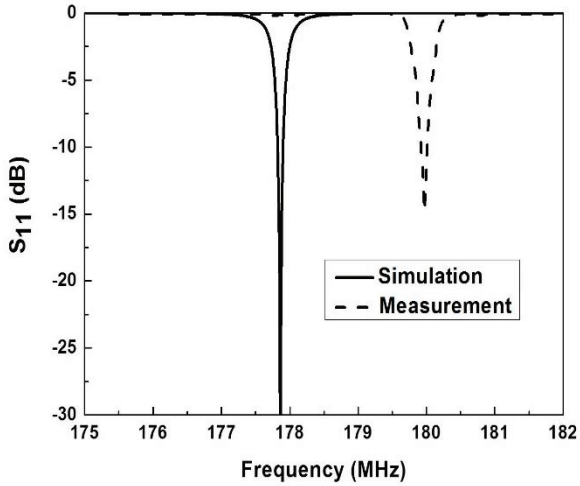

Fig. 12. Measured and simulated reflection coefficients of evolved ENG ZOR antenna.

V. CONCLUSION

An evolved ENG ZOR patch antenna with miniaturized size and ultra-low profile is proposed in this paper. With the aid of equivalent circuit models, the ZOR operational frequency could drop from 5.084 GHz to 177.8685 MHz by modifying an ordinary ENG ZOR by steps. The radiation performance with miniaturized size enables it applicable for the specified low-power radio applications, such as short range remote control system, household security system and so on. As a future work, benefiting from so wide tunable frequency range for such miniature antenna design, DC-bias diode is planned to be implemented into such antenna design to obtain wideband frequency-agile function [38] and the possibility is now under consideration.

ACKNOWLEDGMENT

This work was supported by the Fundamental Research Foundation for the Central Universities (Grant No. CDJZR12165501) and by Natural Science Foundation of Chongqing, China (Grant No. CSTC2013JJB40005).

REFERENCES

[1] H. A. Wheeler, "Fundamental limitations of small antennas," *Proc. IRE*, vol. 35, pp. 1479-1484, 1947.

[2] L. J. Chu, "Physical limitation on omni-directional antennas," *J. Appl. Phys.*, vol. 19, pp. 1163-1175, 1948.

[3] E. E. Altshuler, "Electrically small self-resonant wire antennas optimized using a genetic algorithm," *IEEE Trans. Antennas Propag*., vol. 50, pp. 297-300, 2002.

[4] H. Choo and H. Ling, "Design of electrically small planar antennas using inductively coupled feed," *Electron. Lett.*, vol. 39, pp. 1563-1565, 2003.

[5] S. Kashihara and F. Kuroki, "Bilaterally-etched cross meander-line as an electrically-small antenna at VHF band," *In Proc. China-Japan Joint Micro. Conf.*, Shanghai, China, pp. 144-146, September 2008.

[6] T. Terada, K. Ide, K. Iwata, and T. Fukusako, "Design of a small, low-profile print antenna using a Peano line," *Microw. Opt. Technol. Lett.*, vol. 51, pp. 1833-1838, 2009.

[7] R. Azadegan and K. Sarabandi, "A novel approach for miniaturization of slot antennas," *IEEE Trans. Antennas Propag.*, vol. 51, pp. 421-429, 2003.

[8] K. Sarabandi and R. Azadegan, "Design of an efficient miniaturized UHF planar antenna," *IEEE Trans. Antennas Propag.*, vol. 51, pp. 1270-1276, 2003.

[9] N. Behdad and K. Sarabandi, "Bandwidth enhancement and further size reduction of a class of miniaturized slot antennas," *IEEE Trans. Antennas Propag.*, vol. 52, pp. 1928-1935, 2004.

[10] Y. Tikhov, Y. Kim, and Y. H. Min, "Planar radiator with refined slot pattern for electrically small antennas," *IEEE Proc. Microw. Antennas Propag.*, vol. 153, pp. 19-24, 2006.

[11] K. V. Caekenberghe, N. Behdad, K. M. Brakora, and K. Sarabandi, "A 2.45-GHz electrically small slot antenna," *IEEE Antennas Wireless Propag. Lett.*, vol. 7, pp. 346-348, 2008.

[12] W. Hong and K. Sarabandi, "Low profile miniaturized planar antenna with omnidirectional vertically polarized radiation," *IEEE Trans. Antennas Propag.*, vol. 56, pp. 1533-1540, 2008.

[13] H. R. Stuart and A. Pidwerbetsky, "Electrically small antenna elements using negative permittivity resonators," *IEEE Trans. Antennas Propag.*, vol. 54, pp. 1644-1653, 2006.

[14] R. W. Ziolkowski and A. Erentok "Metamaterial-based efficient electrically small antennas," *IEEE Trans. Antennas Propag.*, vol. 54, pp. 2113-2130, 2006.

[15] S. Ghadarghadr, A. Ahmadi, and H. Mosallaei, "Negative permeability-based electrically small antennas," *IEEE Antennas Wireless Propag. Lett.*, vol. 7, pp. 13-17, 2008.

[16] C. C. Lin, R. W. Ziolkowski, J. A. Nielsen, M. H. Tanielian, and C. L. Holloway, "An efficient, low profile, electrically small, three-dimensional, very high frequency magnetic EZ antenna," *Appl. Phys. Lett*., vol. 96, pp. 104102 (1-3), March 2010.

[17] K. Z. Rajab, R. Mittra, and M. T. Lanagan, "Size reduction of microstrip patch antennas with left-handed transmission line loading," *IET Microw. Antennas Propag.*, vol. 1, pp. 39-44, 2007.

[18] K. Y. Hui and K. M. Luk, "A miniature dielectric resonator loaded patch antenna," *IEEE Trans. Antennas Propag.*, vol. 53, pp. 2118-2122, 2005.

[19] K. D. Jang, J. H. Kim, D. H. Lee, G. H. Kim, W. M. Seong, and W. S. Park, "A small CRLH-TL metamaterial antenna with a magneto-dielectric material," *IEEE AP-S Int. Antennas Propag. Symp. Dig.*, San Diego, USA, pp. 1-4, 2008.

[20] M. E. Emutlu, C. R. Simovski, M. K. Kärkkäinen, P. Ikonen, S. A. Tretyakov, and A. A. Sochava, "Miniaturization of patch antennas with new artificial magnetic layers," *Antenna Technology: Small Antennas and Novel Metamaterials, 2005. IWAT 2005. IEEE International Workshop*, pp. 87-90, March 2005.

[21] P. Y. Chen and A. Alù, "Sub-wavelength elliptical patch antenna loaded with μ-negative metamaterials," *IEEE Trans. Antennas Propag.*, vol. 58, pp. 2909-2919, 2010.

[22] M. Li, X. Q. Lin, J. Y. Chin, R. Liu, and T. J. Cui, "A novel miniaturized printed planar antenna using split-ring resonator," *IEEE Antennas Wireless Propag. Lett.*, vol. 7, pp. 629-631, 2008.

[23] Y. Kim, J. Kim, J. Kim, H. Kim, and H. Lee, "Negative permeability metamaterial structure based electrically small loop antenna," *Advanced Communication Technology, 2008. ICACT 2008. 10th International Conference*, Phoenix Park, Korea, pp. 769-773, 2008.

[24] A. Lai, K. M. K. H. Leong, and T. Itoh, "Infinite wavelength resonant antennas with monopolar radiation pattern based on periodic structures," *IEEE Trans. Antennas Propag.*, vol. 55, pp. 868-876, 2007.

[25] S. Pyo, S.-M. Han, J. W. Baik, and Y. S. Kim, "A slot-loaded composite right/left-handed transmission line for a zeroth-order resonant antenna with improved efficiency," *IEEE Trans. Microw. Theory Tech.*, vol. 57, pp. 2775-2782, 2009.

[26] Y. Dong and T. Itoh, "Miniaturized substrate integrated waveguide slot antennas based on negative order resonance," *IEEE Trans. Antennas Propag.*, vol. 58, pp. 3856-3864, 2010.

[27] S. W. Lee and J. H. Lee, "Electrically small MNG ZOR antenna with multilayered conductor," *IEEE Antennas Wireless Propag. Lett.*, vol. 9, pp. 724-727, 2010.

[28] J. H. Park, Y. H. Ryu, J. G. Lee, and J. H. Lee,

"Epsilon negative zeroth-order resonator antenna," *IEEE Trans. Antennas Propag.*, vol. 55, pp. 3710-3712, 2007.

[29] W. C. Chang and B. Lee, "Wideband one-unit-cell ENG zeroth-order resonant antenna," *Electron. Lett.*, vol. 45, pp. 1289-1291, 2009.

[30] S. Jang and B. Lee, "Meta-structured one-unit-cell epsilon negative antenna," *Microw. Opt. Technol. Lett.*, vol. 51, pp. 2991-2994, 2009.

[31] J. Kim, G. Kim, W. Seong, and J. Choi, "A tunable internal antenna with an epsilon negative zeroth order resonator for DVB-H service," *IEEE Trans. Antennas Propag.*, vol. 57, pp. 4014-4017, 2009.

[32] J. Q. Huang and Q. X. Chu, "Small ZOR antenna with high efficiency based on epsilon negative transmission line," *2010 IEEE Microwave and Millimeter Wave Technology (ICMMT), 2010 International Conference*, Chengdu, China, pp. 1905-1907, 2010.

[33] "Ansoft high frequency structure simulation (HFSS)," ver. 10, *Ansoft Corp*., 2005.

[34] A. Sanada, M. Kimura, I. Awai, C. Caloz, and T. Itoh, "A planar zeroth-order resonator antenna using a left-handed transmission line," *In Proc. Eur. Microwave Conf.*, pp. 1341-1344, 2004.

[35] J. Rashed and C. T. Tai, "A new class of resonant antennas," *IEEE Trans. Antennas Propag.*, vol. 39, pp. 1428-1430, 1991.

[36] T. J. Warnagiris and T. J. Minardo, "Performance of a meandered line as electrically small transmitting antenna," *IEEE Trans. Antennas Propag.*, vol. 46, pp. 1797-1876, 1998.

[37] G. Marrocco, "Gain-optimized self-resonant meander line antennas for RFID applications," *IEEE Antennas Wireless Propag. Lett.*, vol. 2, pp. 302-305, 2003.

[38] M. C. Tang and R. W. Ziolkowski, "A frequency agile, ultralow-profile, complementary split ring resonator-based electrically small antenna," *Microw. Opt. Technol. Lett.*, vol. 55, pp. 2425-2428, 2013.